DOC2b Enhances β-Cell Function via a Novel Tyrosine Phosphorylation-Dependent Mechanism

Diti Chatterjee Bhowmick,[1] Arianne Aslamy,[2] Supriyo Bhattacharya,[3] Eunjin Oh,[1] Miwon Ahn,[1] and Debbie C. Thurmond[1]

Diabetes 2022;71:1246–1260 | https://doi.org/10.2337/db21-0681

Double C2 domain B (DOC2b) protein is required for glucose-stimulated insulin secretion (GSIS) in β-cells, the underlying mechanism of which remains unresolved. Our biochemical analysis using primary human islets and human and rodent clonal β-cells revealed that DOC2b is tyrosine phosphorylated within 2 min of glucose stimulation, and Src family kinase member YES is required for this process. Biochemical and functional analysis using DOC2b^{Y301} mutants revealed the requirement of Y301 phosphorylation for the interaction of DOC2b with YES kinase and increased content of VAMP2, a protein on insulin secretory granules, at the plasma membrane (PM), concomitant with DOC2b-mediated enhancement of GSIS in β-cells. Coimmunoprecipitation studies demonstrated an increased association of DOC2b with ERM family proteins in β-cells following glucose stimulation or pervanadate treatment. Y301 phosphorylation-competent DOC2b was required to increase ERM protein activation, and ERM protein knockdown impaired DOC2b-mediated boosting of GSIS, suggesting that tyrosine-phosphorylated DOC2b regulates GSIS via ERM-mediated granule localization to the PM. Taken together, these results demonstrate the glucose-induced posttranslational modification of DOC2b in β-cells, pinpointing the kinase, site of action, and downstream signaling events and revealing a regulatory role of YES kinase at various steps in GSIS. This work will enhance the development of novel therapeutic strategies to restore glucose homeostasis in diabetes.

Glucose-stimulated insulin secretion (GSIS) from β-cells occurs in two distinct phases. The transient first phase of insulin secretion occurs within 10 min of glucose stimulation via the stimulus-secretion coupling pathway (1,2). This pathway begins with the entry of extracellular glucose into the β-cell, metabolism of glucose to yield an elevated ATP/ADP ratio, which triggers closure of ATP-sensitive potassium channels and subsequent plasma membrane (PM) depolarization, evoking an influx of calcium through voltage-gated calcium channels and a burst of insulin granule fusion and insulin release (1–4). The second phase of insulin secretion begins during the first phase and persists until normoglycemia is restored (5). The second phase of insulin secretion can persist as a result of the mobilization of insulin secretory granules (SGs) from the reserve pools deep within the cell to the PM, which requires remodeling of the actin cytoskeleton (5–9). The distal steps of insulin granule exocytosis and insulin release are regulated by the soluble *N*-ethylmaleimide–sensitive factor attachment protein receptor (SNARE) proteins (10,11). SNARE complex assembly in the β-cell is further regulated by accessory binding proteins, such as double C2 domain B (DOC2b) (12–15). However, the detailed molecular events involving DOC2b in regulating biphasic insulin secretion remain unclear.

DOC2b, a member of the double C2 domain protein family, is a ubiquitously expressed 46–50-kDa protein composed of an N-terminal Munc13-interacting domain and C-terminal tandem C2 domains (C2A and C2B) (13,16,17). The C2 domains are known to bind calcium and phospholipids (18,19) and, in the context of spontaneous neurotransmitter release, confer DOC2b's required role as a calcium sensor (19–21). In addition to neuronal defects, islets isolated from whole-body DOC2b knockout mice show loss of biphasic insulin release (15,22), consistent with islet β-cells being closely functionally related to

[1]Department of Molecular and Cellular Endocrinology, Diabetes and Metabolic Research Institute, Beckman Research Institute of City of Hope, Duarte, CA
[2]Department of Medicine, Cedars-Sinai Medical Center, West Hollywood, CA
[3]Department of Computational and Quantitative Medicine, City of Hope, Duarte, CA

Corresponding author: Debbie C. Thurmond, dthurmond@coh.org

Received 2 August 2021 and accepted 13 March 2022

This article contains supplementary material online at https://doi.org/10.2337/figshare.19411307.

neuroendocrine cells. Furthermore, low DOC2b transcript levels have been observed in cultured islet β-cells from humans and rodents with diabetes (12,23). In contrast, islets from an early line of "global" DOC2b-overexpressing transgenic mice (tet-off system; TRE promoter and CMV minimal promoter-driven transgene) showed boosted biphasic glucose-stimulated insulin release ex vivo, implicating DOC2b in this process as having therapeutic potential (17). However, DOC2b's impact in other cell types involved in metabolism was a confounding factor in this global model, as was the expression of the transgene during pancreatic development (17). Subsequent determination of boosted biphasic insulin release in an inducible β-cell–specific DOC2b transgenic mouse model pointed to a specific and beneficial role for DOC2b enrichment in the adult mouse β-cell (24). In addition, these mice were protected from diabetogenic stimuli, indicating physiologic relevance for DOC2b enrichment as a potential therapeutic opportunity (24).

The Sec/Munc18 protein Munc18c is operational in second-phase insulin release and directly associates with the C2B domain of DOC2b at the PM of the β-cell, and this association is essential for SNARE-mediated insulin granule exocytosis (13). The N-terminal Munc13-interacting domain is dispensable for mediating DOC2b boosting of GSIS, while the tandem C2 domains (referred to as C2AB) fully accounted for the GSIS boosting effect and conferred protection from diabetogenic stimuli (24). While yet unexplored in β-cells, the phosphorylation of DOC2b regulates GLUT4 vesicle mobilization in skeletal muscle cells in a cytoskeletal-based mechanism via interaction with KLC1 (25). DOC2b also binds to other cytoskeletal factors (26–28), although whether DOC2b is operational in cytoskeletal remodeling in the β-cell remains unknown.

YES kinase, a member of the nonreceptor protein-tyrosine Src family kinase (SFK), is rapidly phosphorylated at the PM yet operational largely in second-phase GSIS via insulin granule mobilization involving F-actin remodeling in the β-cell (29). Based on this, in the current study, we hypothesized that glucose stimulation would phosphorylate DOC2b at one or more tyrosine residues located in the C2B domain, via an SFK-dependent mechanism, to promote insulin granule localization at the PM and boost SNARE-mediated insulin exocytosis from β-cells. In this study, we have tested this hypothesis using DOC2b-overexpressing human islets and human and mouse clonal β-cell lines.

RESEARCH DESIGN AND METHODS

Plasmids and Adenovirus Constructs

The adenoviruses Ad.GFP, Ad.rDOC2b-GFP^{WT}, and Ad.rDOC2b-GFP^{Y301F} were generated by inserting GFP, rDOC2b-GFP^{WT}, or rDOC2b-GFP^{Y301F} fusion genes into the viral vector pAd5CMVmpA, respectively, by ViraQuest (North Liberty, IA), as described (25). The rDOC2b-GFP^{Y301E} was generated using site-directed mutagenesis of Y301 to E301 (GenScript, Piscataway, NJ). All of the constructs were confirmed by sequencing. Adenovirus (Ad.) human (h)DOC2B-MYC-DDK^{WT} [DDK is an epitope (FLAG) tag] was generated as described previously (24,25).

Cell Culture, siRNA Transfection, and Insulin Secretion Assays

The cell culture methods for MIN6 β-cells and human pancreatic islets have been described previously (29). Human islets were obtained from the Integrative Islet Distribution Program and City of Hope Islet Cell Resource Center (Supplementary Table 1). EndoC-βH1 cells obtained from Dr. Roland Stein (Vanderbilt University) were cultured as described previously (30). The SFK inhibitor SU6656 (catalog number 572635; EMD Millipore), the tyrosine phosphatase inhibitor pervanadate (pV; freshly made), and/or glucose were incubated with the cells as indicated in the figure legends. The siRNA oligonucleotides (25 nmol/L YES, J-040156–07, ON-TARGETplus, Thermo Dharmacon; 25 nmol/L radixin, L-047230-01-0005, ON-TARGETplus, Thermo Dharmacon; and control: catalog number 1027281, Qiagen) were transfected into MIN6 β-cells using Lipofectamine 2000 and assessments made 48 h later. For insulin secretion assays, MIN6 β-cells were incubated in serum- and glucose-free modified Krebs-Ringer bicarbonate buffer containing 1% radioimmunoassay-grade BSA for 2 h, stimulated with 20 mmol/L glucose (30 min) or 40 mmol/L KCl (15 min) (29). For static GSIS, human islets were preincubated in Krebs-Ringer bicarbonate buffer in low glucose (2.8 mmol/L) for 2 h. Incubation of 10 islets/experimental group (in triplicate) in low or high glucose (16.7 mmol/L) for 2 h was followed by insulin quantification in buffer and cell pellets using a Mouse Insulin ELISA (catalog number 80-INSMSH-E01; Alpco, Salem, NH), human insulin radioimmunoassay (catalog number HI-14K; Millipore), or human insulin ELISA (catalog number 10-1113-01; Mercodia) as indicated in the figure legends. At least three independent human islet donor batches were used in each assay.

Plasmid Transfection and Adenoviral Transduction

MIN6 β-cells were transfected with rDOC2b-GFP^{WT} or rDOC2b-GFP$^{Y301F/E}$ plasmids using Lipofectamine 2000 (Invitrogen) and harvested after 48 h using 1% Nonidet P-40 lysis buffer (29) for downstream analysis. For experiments using adenoviruses, EndoC-βH1 cells, human islets, or MIN6 β-cells cultured in respective growth media were transduced for 1 h (multiplicity of infection 100), washed with the complete growth media twice, and cultured in growth media for an additional 48 h at 37°C. Transduced EndoC-βH1 cells or human islets were harvested using 1% Nonidet P-40 lysis buffer for downstream analysis.

A

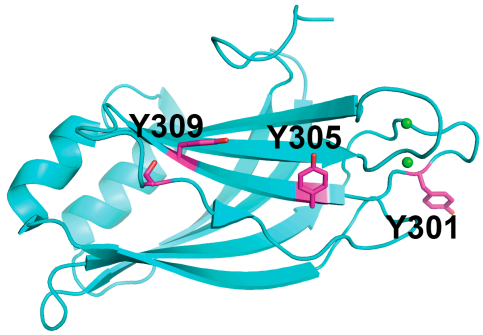

B

Percent Identity Matrix	Human DOC2b	Mouse DOC2b	Rat DOC2b
Human DOC2b	100	95.15	95.39
Mouse DOC2b	95.15	100	98.30
Rat DOC2b	95.39	98.30	100

Percent Identity Matrix	Human C2B	Mouse C2B	Rat C2B
Human C2B	100	98.10	98.10
Mouse C2B	98.10	100	100
Rat C2B	98.10	100	100

C

```
Human   NHTKTFSICLEKQLPVDKTEDKSLEERGRILISLKYSSQKQGLLVGIVRCAHLAAMDANG 300
Mouse   NHTKTFSICLEKQLPVDKAEDKSLEERGRILISLKYSSQKQGLLVGIVRCAHLAAMDANG 300
Rat     NHTKTFSICLEKQLPVDKAEDKSLEERGRILISLKYSSQKQGLLVGIVRCAHLAAMDANG 300
        ******************:************************************

Human   YSDPYVKTYLRPDVDKKSKHKTAVKKKTLNPEFNEEFCYEIKHGDLAKKSLEVTVWDYDI 360
Mouse   YSDPYVKTYLKPDVDKKSKHKTAVKKKTLNPEFNEEFCYEIKHGDLAKKTLEVTVWDYDI 360
Rat     YSDPYVKTYLKPDVDKKSKHKTAVKKKTLNPEFNEEFCYEIKHGDLAKKTLEVTVWDYDI 360
        **********:*************************************:**********

Human   GKSNDFIGGVVLGIHAKGERLKHWFDCLKNKDKRIERWHTLTSELPGAVLSD 412
Mouse   GKSNDFIGGVVLGINAKGERLKHWFDCLKNKDKRIERWHTLTNELPGAVLSD 412
Rat     GKSNDFIGGVVLGINAKGERLKHWFDCLKNKDKRIERWHTLTNEIPGAVLSD 412
        **************:***************************.*:*******
```

D Non-diabetic Human islet

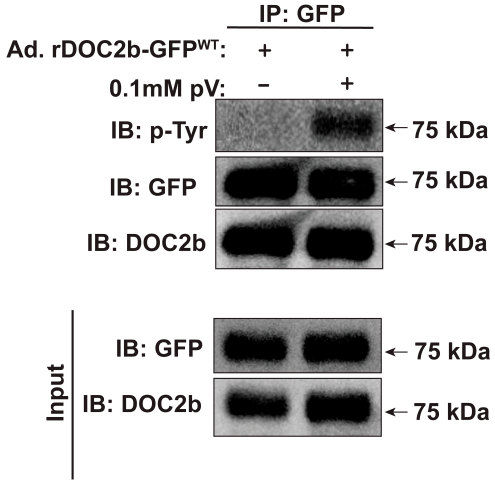

E MIN6 β-Cell

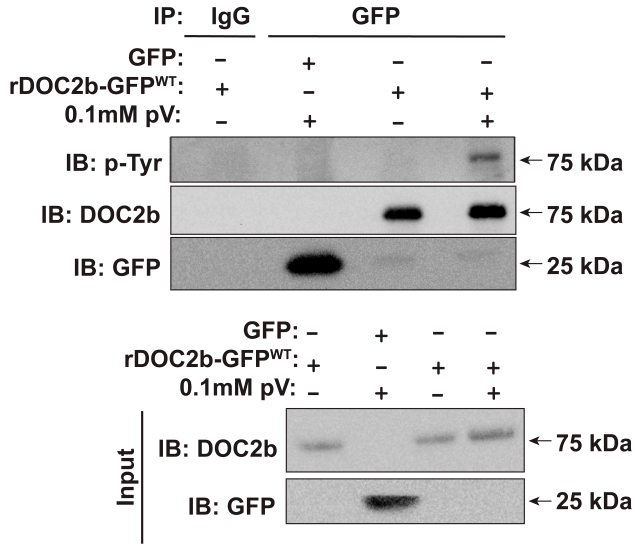

Figure 1—DOC2b is tyrosine phosphorylated in the β-cell. *A*: Predicted structure of rat DOC2b showing the C2B domain with the three putative tyrosine phosphorylation sites. *B*: Percent identity matrix for human, mouse, and rat full-length DOC2b (top panel) and C2B domain (bottom panel). *C*: Multiple sequence alignment of human, rat, and mouse DOC2b using Clustal Omega multiple sequence alignment tool (EMBL-European Bioinformatics Institute). Boxes highlight the conserved amino acid residues in the C2B domain. *D*: DOC2b tyrosine phosphorylation level in Ad.DOC2b-GFP^{WT}-transduced nondiabetic human islets after pV treatment (0.1 mmol/L, 5 min) followed by IP and immunoblot (IB) analysis. *E*: The DOC2b tyrosine phosphorylation level in the GFP/DOC2b-GFP^{WT}-transfected MIN6 β-cells after pV (0.1 mmol/L, 5 min) treatment followed by IP and IB analysis. Data are representative of three independent experiments.

Immunoblotting

Proteins were resolved by 10% or 15% SDS-PAGE and transferred to polyvinylidene fluoride membranes for immunoblotting. The rabbit polyclonal DOC2b primary antibody used was custom developed against the DOC2b 96–119-aa (PSPGPSPARPPAKPPEDEPDA) peptide sequence (custom synthesized by Pacific Immunology Corp.). pSrc antibodies from Cell Signaling Technology detect other SFKs and are thus referred to as phospho-SFK (pSFK). Detailed information about the primary antibodies is provided (Supplementary Table 2). Goat anti-mouse and anti-rabbit horseradish peroxidase secondary antibodies were obtained from Bio-Rad Laboratories and used at 1:5,000. Immunoreactive bands were visualized with ECL, ECL Prime, or ECL Super-Signal reagents (GE Healthcare) and imaged using the Chem-iDoc gel documentation system (Bio-Rad Laboratories). Block-PO Reagent (Millipore) was used to reduce noise in the phospho-specific blots.

Coimmunoprecipitation

Cleared detergent-solubilized lysate protein (2 mg) was immediately incubated for 2 h or overnight with rabbit polyclonal anti-GFP antibody conjugated to Sepharose beads (catalog number ab69314; Abcam) or mouse anti-MYC antibody conjugated to agarose beads (catalog number ab1253; Abcam) rotating at 4°C. Rabbit IgG (Santa Cruz Biotechnology) was used as a negative control. Coimmunoprecipitated (co-IP) proteins were resolved using SDS-PAGE analyses and immunoblotting.

Molecular Dynamics Simulation Analysis

The initial structure of the rat DOC2b was modeled based on the crystal structures of the rat C2A (Protein Database identification number: 4LCV) and C2B (Protein Database identification number: 4LDC) domains (31). The flexible loop connecting these two domains was modeled using the Protein preparation wizard in Schrodinger Maestro (32). The human DOC2b structure was obtained by aligning the human with the mouse sequence and mutating those positions where the mouse and the human sequences differ. The mutations were performed using the Prime module in Maestro (33). The protein structures were solvated in an explicit water box, and ions were added to neutralize the net charge. The system was parameterized using the ff14SB force field for protein (34) and TIP4PEW force field for water (35). Following minimization using the conjugate gradient method, the system was gradually heated from 0 K to 310 K over 30 ns at constant volume, with harmonic restraints applied to the protein heavy atoms. Next, equilibration was carried out at a constant pressure of 1 atm for 50 ns, while the harmonic restraints were gradually relaxed to zero. Following this, an additional 50 ns of equilibration was performed without any restraints. Five independent simulations (310 K and 1 atm) were performed on each equilibrated structure (i.e., the rat and human DOC2b) starting with random velocities, each simulation lasting for 2.5 μs. Data from all five simulations were aggregated to obtain statistics on the C-terminal distance and solvent-accessible surface areas. The simulations were performed using the GPU (graphics processing unit) accelerated version of AMBER18 (36). The subsequent analysis was performed using CPPTRAJ (37).

Statistical Analysis

All results were evaluated for statistical significance using an unpaired two-tailed Student *t* test for comparison of two groups or ANOVA for more than two groups using Prism version 8.0 (GraphPad Software, La Jolla, CA). Data are expressed as the mean ± SEM.

Data and Resource Availability

The data sets generated during and/or analyzed during the current study are available from the corresponding author upon reasonable request. No applicable resources were generated during this study.

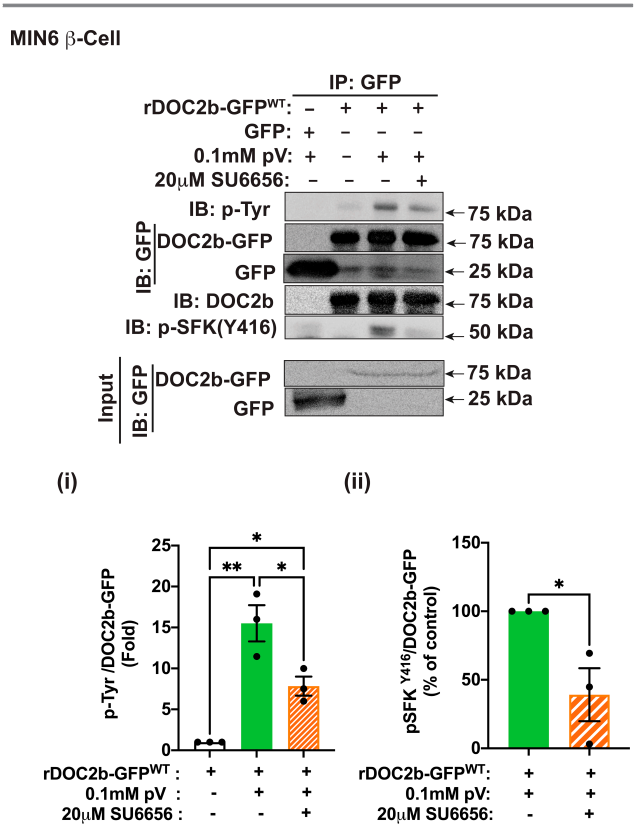

Figure 2—SFK activity is required for the tyrosine phosphorylation of the DOC2b in MIN6 β-cells. Top panel: Representative Western blot images of MIN6 β-cells transfected with either GFP or rDOC2b-GFP^{WT} plasmids and treated with 0.1 mmol/L pV (5 min) with or without 20 μmol/L SU6656 pretreatment (2 h) followed by IP and immunoblot (IB) analysis. Bottom panel: Quantification of the IBs pTyr/DOC2b-GFP (i) and p-SFK^{Y416}/DOC2b-GFP (ii) interactions from three independent experiments using different passages of cells. Data are shown as mean ± SEM. *$P < 0.05$; **$P < 0.002$.

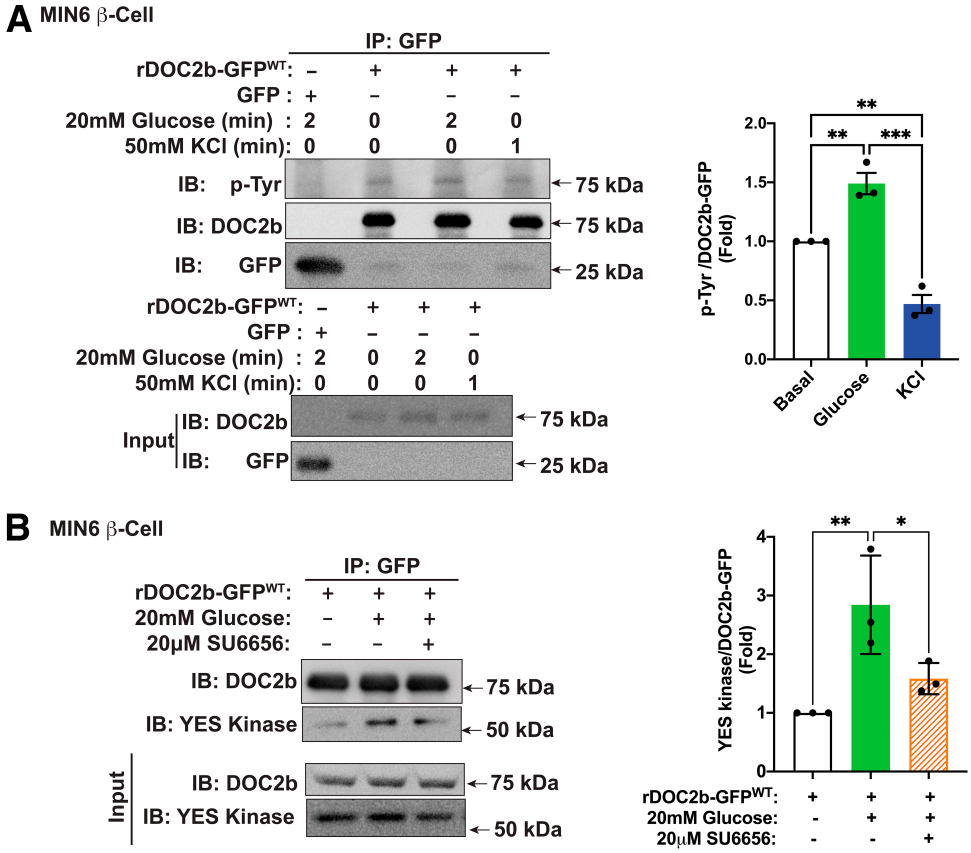

Figure 3—Glucose stimulation augments DOC2b tyrosine phosphorylation and interaction with YES kinase in MIN6 β-cells. *A*, left: Representative Western blot images of DOC2b-GFP^{WT}–transfected MIN6 β-cells treated with either 20 mmol/L glucose for 2 min or 50 mmol/L KCl for 1 min followed by IP and immunoblot (IB). *A*, right: Quantification of the IBs from three independent experiments. *B*, left: Representative Western blot images of MIN6 β-cells transfected with rDOC2b-GFP^{WT} plasmid and stimulated with 20 mmol/L glucose (2 min) with or without 20 μmol/L SU6656 pretreatment (2 h) followed by IP and IB analysis. *B*, right: Quantification of the IBs from three independent experiments. Data are shown as mean ± SEM. *$P < 0.05$; **$P < 0.002$; ***$P < 0.0002$.

RESULTS

DOC2b Undergoes Tyrosine Phosphorylation in Human Islets and β-Cells

DOC2b enrichment in the β-cell enhances GSIS, and the region containing the tandem C2 domains (C2AB) of DOC2b is sufficient to exert this beneficial function (24). The C2B domain of DOC2b harbors three putative tyrosine phosphorylation sites (Y301, Y305, and Y309) (Fig. 1*A*). Multiple alignments of the human, mouse, and ratDOC2b protein revealed >95% and >98% sequence identity for full-length DOC2b (Fig. 1*B*) and the C2B domain, respectively (Fig. 1*B* and *C*). To evaluate if DOC2b undergoes tyrosine phosphorylation in β-cells, we treated nondiabetic human islets transduced to express rDOC2b-GFP^{WT} with or without the tyrosine phosphatase inhibitor pV (38). The use of a DOC2b-GFP fusion protein was required since no custom or commercially available anti-DOC2b antibodies sufficed for IP. DOC2b-GFP and immunoblot for tyrosine-phosphorylated (pTyr) showed a pV-induced increase in pTyr-DOC2b-GFP^{WT} (Fig. 1*D*).

Human islets are composed of multiple cell types, with ∼50–60% being β-cells. To evaluate the phosphorylation of DOC2b in β-cells only, MIN6 β-cells were used. Similar to human islets, pV-induced increase in pTyr-DOC2b-GFP^{WT} was observed in MIN6 β-cells (Fig. 1*E*). Using phospho-protein enrichment analysis as a second approach for validation, MIN6 β-cells were transfected with GFP or rDOC2b-GFP^{WT} and treated with pV. Phospho-enrichment beads captured DOC2b-GFP (75 kDa) and pV stimulation again increased DOC2b phosphorylation (Supplementary Fig. 1) with a magnitude similar to the IP experiments. Glucose stimulation also increased DOC2b phosphorylation relative to basal levels (Supplementary Fig. 1), suggesting that DOC2b undergoes glucose-stimulated tyrosine phosphorylation in β-cells and may be important for the mechanistic connection between DOC2b and GSIS.

Tyrosine-Phosphorylated DOC2b Associates With Activated SFK in β-Cells

Bioinformatic analyses using ExPASy–NetPhos-3.1 and NetworKIN identified SFKs as among the probable kinases

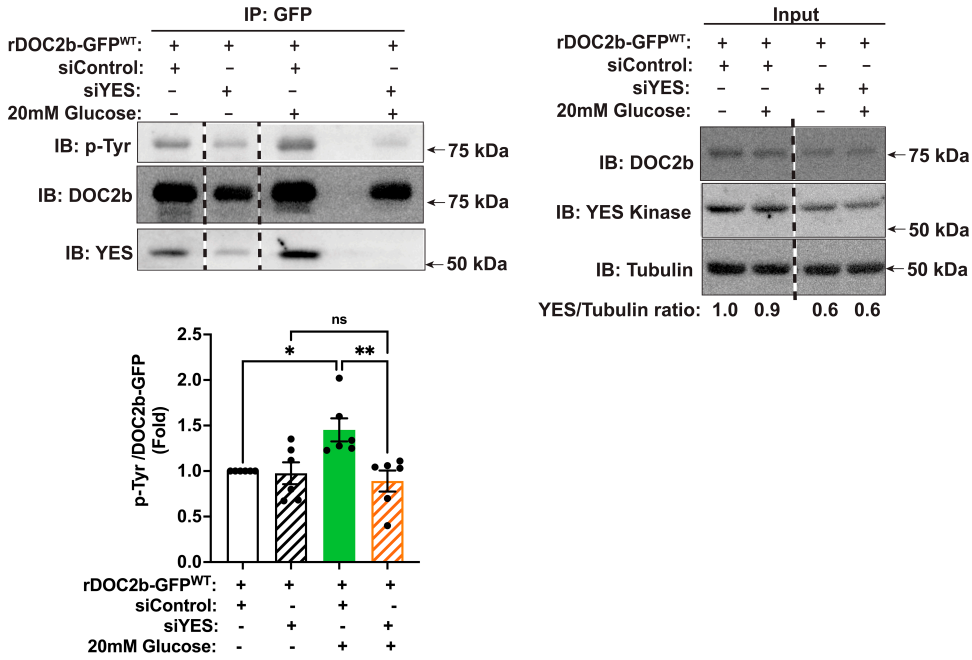

Figure 4—YES kinase knockdown ablates tyrosine phosphorylation of DOC2b in MIN6 β-cells. Representative Western blot images of MIN6 β-cells transfected with rDOC2b-GFP^{WT} plasmid along with control (siControl) or siYES oligonucleotides. After a 48-h incubation, the cells were preincubated in modified Krebs-Ringer bicarbonate buffer for 2 h and stimulated with 20 mmol/L glucose (2 min) followed by IP and immunoblot (IB) analysis. Vertical dashed lines denote splicing of lanes from within the same gel exposure. YES/tubulin ratios demonstrate ~40% siYES-induced knockdown efficiency. Bar graph quantification of the IBs from six independent experiments. Data are shown as mean ± SEM. *$P < 0.05$; **$P < 0.002$.

for tyrosine phosphorylation of DOC2b. Confocal microscopy data validated prior observation of pV-induced SFK activation (pSFK^{Y416}) at the PM, as well as the presence of YES kinase (the glucose-responsive SFK family member in MIN6 cells [29]) (Supplementary Fig. 2*A*). The SFK inhibitor SU6656 was used to evaluate the requirement for SFK activity for the tyrosine phosphorylation of DOC2b-GFP in MIN6 β-cells (Fig. 2). SU6656 reduced the pV-induced tyrosine phosphorylation of DOC2b (>50%) (Fig. 2i) and decreased interaction of pSFK^{Y416} with DOC2b-GFP (>50%) (Fig. 2ii), consistent with SFK activity being required for the tyrosine phosphorylation of DOC2b in MIN6 β-cells.

Next, the human β-cell line EndoC-βH1 was transduced with Ad.hDOC2b-MYC-DDK^{WT} to evaluate the role of SFK in tyrosine phosphorylation. IP for MYC and immunoblotting for pTyr showed a pV-induced increase in pTyr-hDOC2b-MYC-DDK^{WT} (55 kDa) (Supplementary Fig. 2*B*). SU6656 suppressed the pV-induced tyrosine phosphorylation of DOC2b (>90%) and decreased the association of pSFK^{Y416} with hDOC2b-MYC-DDK^{WT}. Human EndoC-βH1 cells transduced with Ad.rDOC2b-GFP^{WT} also exhibited pV-induced DOC2b tyrosine phosphorylation, which was attenuated by SU6656 (Supplementary Fig. 2*C*). These results demonstrate an evolutionarily conserved functional role for SFK in the tyrosine phosphorylation of DOC2b in β-cells.

YES Kinase Is Required for Glucose-Stimulated Tyrosine Phosphorylation of DOC2b in β-Cells

We have previously demonstrated that within the nine-member SFK family, only Src, Fyn, and YES proteins are detectable in β-cells, and only YES is tyrosine phosphorylated in response to glucose at the PM in the β-cell (29). Similar to YES kinase, the increase in DOC2b tyrosine phosphorylation was prompted by glucose stimulation and did not respond to KCl stimulation (Fig. 3*A*). Maximal tyrosine phosphorylation of rDOC2b-GFP^{WT} in response to stimulatory 20 mmol/L glucose was achieved within ~1 to 2 min (Supplementary Fig. 3), at or just following the glucose-induced peak activation of YES kinase at ~1 min (29).

To determine if YES associates with DOC2b in the β-cell following glucose treatment, DOC2b-GFP IP was performed from rDOC2b-GFP^{WT}–transfected MIN6 β-cells. Indeed, immunoblotting confirmed the association of YES with rDOC2b-GFP^{WT} (more than twofold) within 2 min of glucose stimulation (Fig. 3*B*). SU6656 reduced (>40%) the DOC2b-GFP–YES kinase interaction, consistent with YES regulating the glucose-induced tyrosine phosphorylation of DOC2b-GFP (Fig. 3*B*).

Furthermore, using PM and SG fractions, glucose stimulation and pV treatments increased levels of DOC2b-GFP in the PM fraction (>1.5-fold) (Supplementary Fig. 4*A*). To determine localization of the pTyr–DOC2b-GFP, GFP was precipitated from fractions, glucose stimulation and pV-

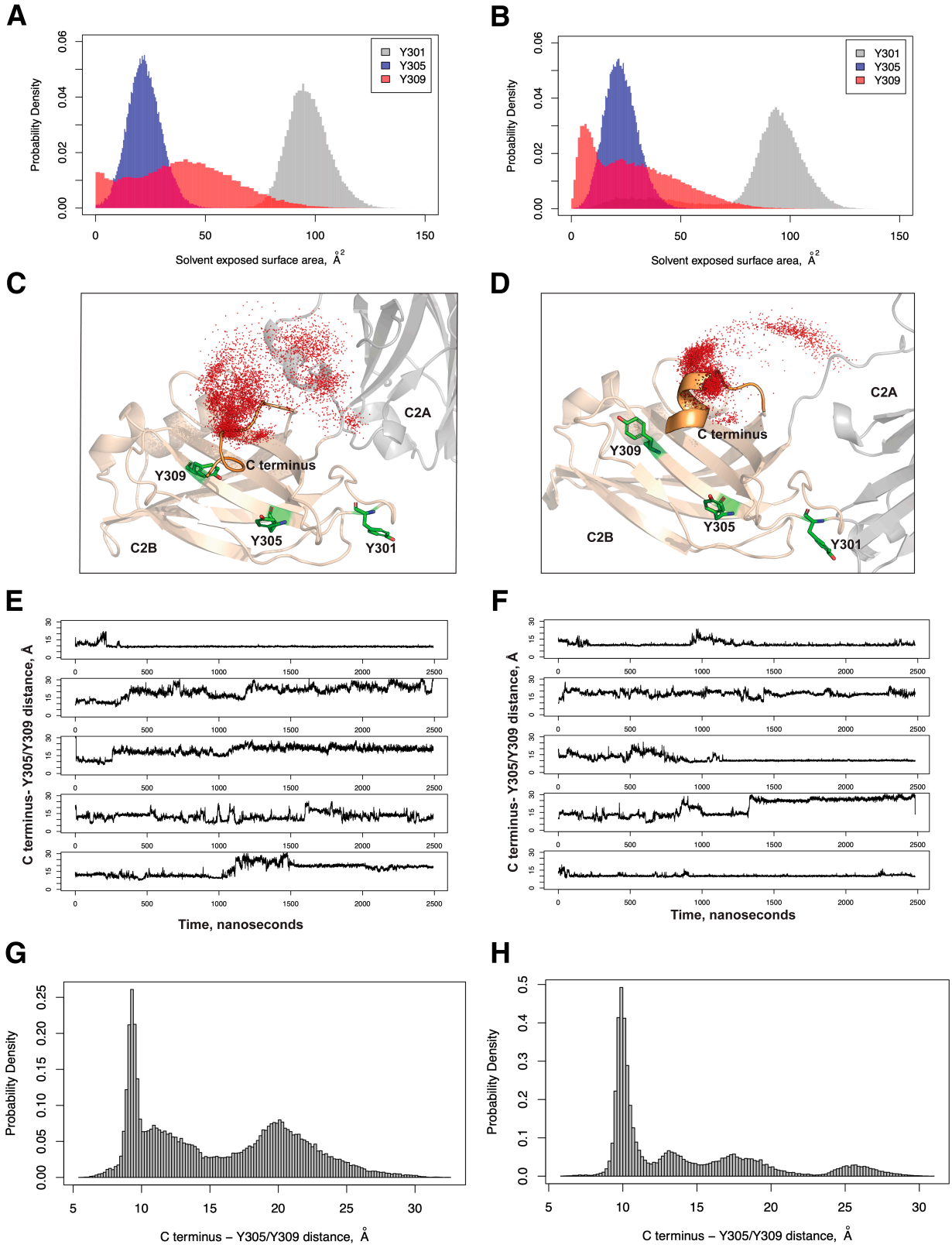

Figure 5—Y301 has a higher solvent-exposed surface area compared with Y305 and Y309 in both rat and human DOC2b. Rat (*A*) and human (*B*) DOC2b MD simulations showing the probability distributions of the solvent-exposed surface areas of Y301, Y305, and Y309. Representative conformations showing the C termini and the C2B domains of rat (*C*) and human (*D*) DOC2b from the highest populated clusters from MD. The C terminus positions from the individual MD frames are shown as red dots. MD simulation data showing rat (*E*) and human (*F*) DOC2b distances from the C terminus to Y305/Y309 with time ($n = 5$ independent MD simulations). The probability distribution of the distance between the rat (*G*) and human (*H*) DOC2b C terminus and Y305/Y309 is shown.

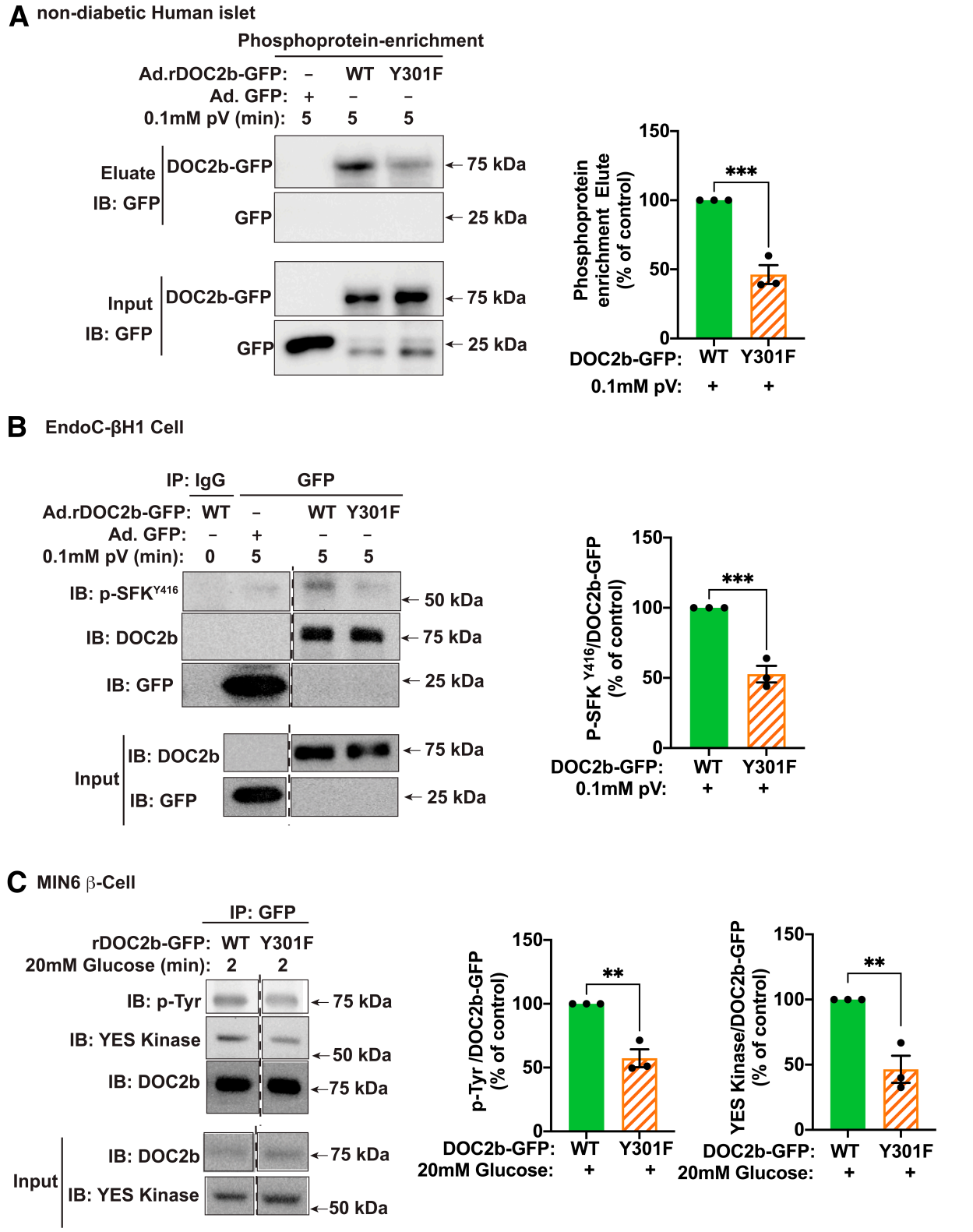

Figure 6—Y301F mutation reduces the tyrosine phosphorylation of DOC2b and blocks its interaction with activated SFK and YES in the β-cell. *A*, left: Representative Western blot images of nondiabetic human islets transduced with Ad.GFP, Ad.rDOC2b-GFP^{WT}, or Ad.rDOC2b-GFP^{Y301F}, incubated for 48 h, and treated with pV (0.1 mmol/L, 5 min) followed by phosphoprotein enrichment and immunoblot (IB) analysis. *A*, right: Quantification of the IBs from three independent experiments. *B*, left: Representative IB images of human EndoC-βH1 cells transduced with Ad.GFP, Ad.rDOC2b-GFP^{WT}, or Ad.rDOC2b-GFP^{Y301F} and treated with or without 0.1 mmol/L pV for 5 min followed by IP and IB analysis. *B*, right: Quantification of the IBs from three independent experiments. *C*, left: Representative Western blot images of MIN6 β-cells transfected with either rDOC2b-GFP^{WT} or rDOC2b-GFP^{Y301F} and stimulated with or without glucose for 2 min followed by IP and IB analysis. Vertical dashed lines denote splicing of lanes from within the same gel exposure. *C*, right: Quantification of the IBs from three independent experiments. Data are shown as mean ± SEM. $^{**}P < 0.002$; $^{***}P < 0.0002$.

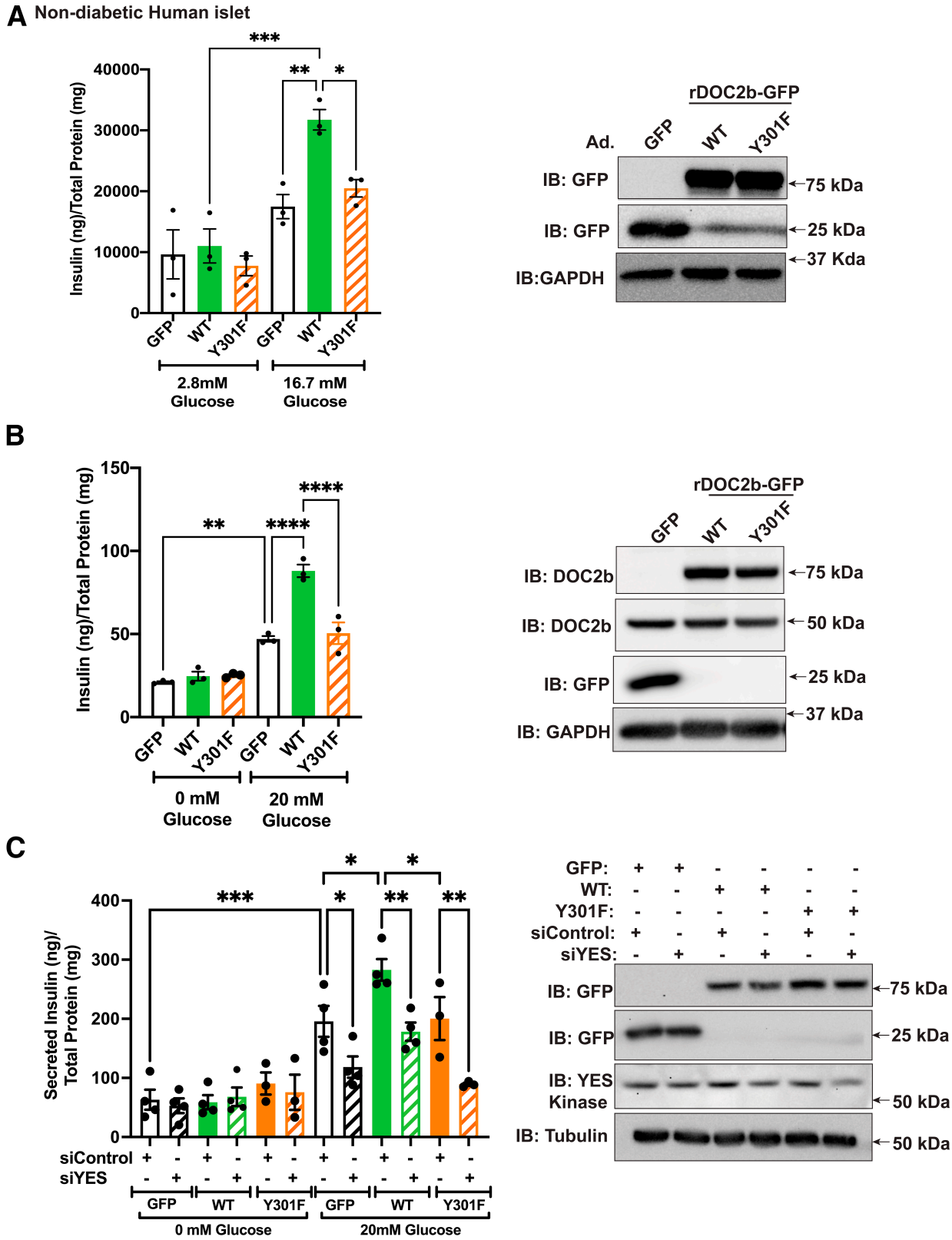

Figure 7—Y301 of DOC2b mediates enhanced GSIS in human islet and rodent β-cells. *A*, left: Static GSIS of nondiabetic human islet cells transduced with Ad.GFP/Ad.rDOC2b-GFP^{WT}/Ad.rDOC2b-GFP^{Y301F}. Glucose stimulation was performed for total 2 h using 10 medium-sized (250–300-μm) islets per experimental group. *A*, right: Representative Western blot images of nondiabetic human islet cells transduced with Ad.GFP/Ad.rDOC2b-GFP^{WT}/Ad.rDOC2b-GFP^{Y301F}. Insulin was quantified using human (catalog number HI-14K; Millipore) insulin radioimmunoassay. *B*, left: GSIS of MIN6 β-cells transfected with GFP, rDOC2b-GFP^{WT}, or rDOC2b-GFP^{Y301F}. Glucose stimulation was performed for 30 min. Insulin was quantified using a Mouse Insulin ELISA (catalog number 80-INSMSH-E01; Alpco). *B*, right:

induced pTyr (≥1.4-fold), and interaction with YES kinase (~3.5-fold) (Supplementary Fig. 4*A*) only from the PM fraction (Supplementary Fig. 4*A*), consistent with the concept of YES kinase phosphorylating DOC2b at the PM.

To determine a requirement for YES kinase for glucose-stimulated tyrosine phosphorylation of DOC2b in β-cells, we selectively depleted YES using RNA interference in MIN6 β-cells. YES siRNA (siYES) reduced the endogenous YES protein level by ~40% (Fig. 4, input fractions lanes 3 to 4), as previously described (29), but did not alter the levels of Src and FYN, the other two members of SFK in the MIN6 β-cell (Supplementary Fig. 4*B*). IP of DOC2b-GFP and immunoblotting for pTyr showed glucose-induced tyrosine phosphorylation of DOC2b-GFP, which was blocked by siYES treatment (Fig. 4). Altogether, these results established the importance of YES for DOC2b's tyrosine phosphorylation following glucose stimulation in β-cells.

DOC2b Y301 Is Required for DOC2b-YES Interaction and Tyrosine Phosphorylation of DOC2b in β-Cells

To investigate the mechanism of DOC2b tyrosine phosphorylation in β-cells, we evaluated which of the tyrosine residues in the C2B domain is necessary for DOC2b phosphorylation and interaction with YES and pSFK^{Y416}. Molecular Dynamics (MD) simulation analysis of rat and human DOC2b revealed a larger solvent-exposed surface area for Y301 than Y305 and Y309, indicating that Y301 is more accessible to kinases and therefore more likely to be phosphorylated than Y305 and Y309 (Fig. 5*A* and *B*). The analysis further showed that in both rat and human DOC2b, Y301 is in a flexible loop, while both Y305 and Y309 are in a folded β-sheet (Fig. 5*C* and *D*). Moreover, Y305 is packed against an adjacent loop in DOC2b, and the flexible C terminus of DOC2b makes frequent contact with both Y305 and Y309 but not with Y301 (which is far from the C terminus) (Fig. 5*C–F* and Supplementary Video 1). These features further reduce the solvent accessibility of Y305 and Y309 and interfere with the ability of tyrosine kinases to access Y305 and Y309. Interestingly, as shown in the distance probability distributions, although the C terminus contacts Y305 and Y309 in both human and rat DOC2b, the contacts are more sustained in humans than rats (Fig. 5*G* and *H*).

Next, we investigated the ability of the phosphodeficient DOC2b^{Y301F} mutant to interact with YES/pSFK^{Y416} in the β-cell. Nondiabetic human islets transduced to express rDOC2b-GFP^{Y301F} showed reduced DOC2b-GFP in phosphoprotein-enriched fractions after pV treatment, compared with islets transduced with DOC2b-GFP^{WT} (Fig. 6*A*). To determine the β-cell as the source of this interaction, co-IP from human EndoC-βH1 cell lysates revealed the requirement for the Y301 site; Y301F mutation (DOC2b-GFP^{Y301F}) exhibited an attenuated association with pSFK^{Y416} compared with that of DOC2b-GFP^{WT} (Fig. 6*B*). The importance of Y301 in the regulation of glucose-stimulated DOC2b-YES association and DOC2b tyrosine phosphorylation was confirmed in mouse MIN6 β-cells (Fig. 6*C*).

DOC2b Y301 and YES Kinase Are Essential for the Boosting of GSIS in β-Cells

We next evaluated the importance of Y301 in the ability of DOC2b to boost GSIS using nondiabetic human islets. Static insulin release assays demonstrated attenuated GSIS boosting in the islets expressing rDOC2b-GFP^{Y301F} compared with cells expressing rDOC2b-GFP^{WT} (Fig. 7*A*). Perifusion studies using nondiabetic human islets revealed marked boosting of both the first and second phases of GSIS by rDOC2b-GFP^{WT} enrichment (Supplementary Fig. 5*A*), supporting previous findings using murine islets (39). This boosting function was significantly dampened by rDOC2b-GFP^{Y301F} enrichment (Supplementary Fig. 5*A*), indicating requirement of Y301 phosphorylation for boosting both the first and second phases of GSIS in β-cells.

Similar outcomes were seen with MIN6 β-cells (Fig. 7*B*). Comparison of the Y301F mutant to WT showed that the mutant failed to elicit boosting; the mutant did not exert dominant-negative actions on endogenous DOC2b. Expression of the rDOC2b-GFP^{WT}, rDOC2b-GFP^{Y301F}, and endogenous DOC2b proteins was similar (Fig. 7*B*). MIN6 β-cells transfected to express a phosphomimetic mutant, rDOC2b-GFP^{Y301E}, exhibited increased basal insulin secretion relative to cells transfected with GFP, rDOC2b-GFP^{WT}, or rDOC2b-GFP^{Y301F} (Supplementary Fig. 5*B–D*), resulting in reduced stimulation index in rDOC2b-GFP^{Y301E} cells.

To evaluate the requirement of YES kinase in the ability of DOC2b to boost GSIS, MIN6 β-cells were depleted of YES using RNA interference. Validating prior results (29), YES depletion significantly reduced GSIS (GFP-MIN6 β-cells) but not KCl-stimulated insulin secretion (Fig. 7*C* and Supplementary Fig. 5*E*). MIN6 cells with siYES plus rDOC2b-GFP^{WT} showed significantly attenuated GSIS as compared with siControl plus rDOC2b-GFP^{WT} cells (Fig. 7*C*), indicating the specific requirement of YES kinase in DOC2b-mediated boosting of GSIS. Reduction of GSIS in the siYES plus rDOC2b-GFP^{Y301F}–enriched cells compared with siControl plus rDOC2b-GFP^{Y301F} cells was observed, yielding GSIS levels similar to those from the GFP plus siYES cells (Fig. 7*C*). Immunoblotting of cell lysates

Representative Western blot images of MIN6 β-cells transfected with GFP, rDOC2b-GFP^{WT}, or rDOC2b-GFP^{Y301F}. *C*, left: GSIS of MIN6 β-cells transfected with siControl or siYES plus GFP, rDOC2b-GFP^{WT}, or rDOC2b-GFP^{Y301F}. Glucose stimulation was performed for 30 min. Insulin was quantified using a Mouse Insulin ELISA (catalog number 80-INSMSH-E01). *C*, right: Representative Western blot images of transfected MIN6 β-cells. Western blot images are representative of three independent experiments. Anti-GAPDH/tubulin antibodies were used as a loading control. Data are shown as mean ± SEM. *$P < 0.05$; **$P < 0.002$; ***$P < 0.0002$; ****$P < 0.0001$.

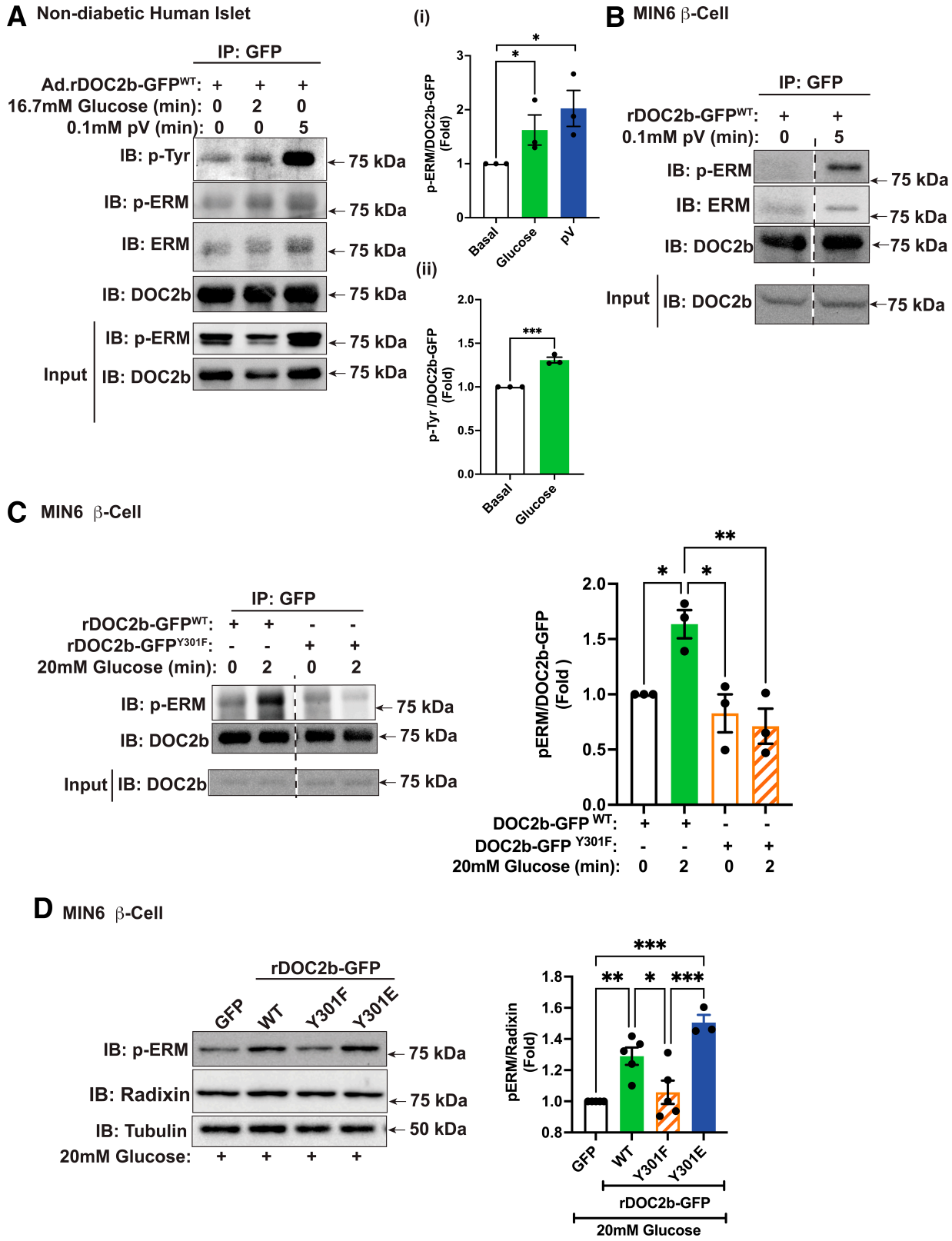

Figure 8—Glucose stimulation and pV treatment augment the binding of DOC2b with p-ERM in β-cells. *A*: Representative Western blot images of nondiabetic human islets transduced with Ad.rDOC2b-GFP^{WT} for 48 h and treated with or without 20 mmol/L glucose (2 min) or 0.1 mmol/L pV (5 min) followed by IP and immunoblot (IB) analysis. *Ai*: p-ERM/DOC2b ratio, quantified from three independent sets of experiments. *Aii*: pTyr/DOC2b ratio, quantified from three independent experiments. *B*: Representative Western blot images of MIN6 β-cells transfected with rDOC2b-GFP^{WT} for 48 h and treated with or without 0.1 mmol/L pV (5 min), followed by IP and IB analysis. Images are representative of three independent experiments using independent passages of cells. *C*, left: Representative IB images of MIN6 β-cells transfected with rDOC2b-GFP^{WT} or rDOC2b-GFP^{Y301F} for 48 h and treated with or without 20 mmol/L glucose (2 min) followed by

showed substantial YES depletion and equivalent expression of the GFP, rDOC2b-GFP^{WT}, and rDOC2b-GFP^{Y301F} proteins (Fig. 7*C*).

We next determined if DOC2b enrichment in β-cells boosts GSIS by impacting the presence of the v-SNARE VAMP2, a protein present on insulin SGs (ISGs), in the PM fraction within 2 to 3 min of glucose stimulation in MIN6 cells, as detected by subcellular fractionation assay (40). VAMP2 levels increased more than fourfold higher in the PM fraction of glucose-stimulated versus unstimulated rDOC2b-GFP^{WT}–enriched MIN6 β-cells, a significant increase compared with that of the GFP control; this increase with WT DOC2b was abrogated by Y301F mutation (Supplementary Fig. 6). These results revealed a positive regulatory role of DOC2b in the β-cell and identified Y301 as a key site for this beneficial effect.

Glucose Stimulation and pV Treatment Augment the Binding of DOC2b With Phosphorylated ERM in the β-Cell

To identify candidate proteins that associate with DOC2b-GFP in β-cells selectively in response to glucose stimulation, we performed mass spectrometry analysis of proteins that co-IP with DOC2b-GFP (Supplementary Fig. 7). The presence of the DOC2b peptide and its known binding partner Munc13-1 verified the reliability of the mass spectrometry analysis; DOC2b was not detected in GFP-expressing co-IPs, and Munc13-1 was selective for DOC2b-GFP IP (Supplementary Table 3). Among the proteins with at least three unique peptides that showed selective binding with DOC2b-GFP, nine proteins were identified based on their potential involvement in actin cytoskeleton remodeling (Supplementary Table 3). Among these nine proteins, the scaffolding proteins ezrin, radixin, and moesin (collectively referred to as ERM proteins) were chosen for further analysis based on their previously reported affiliation with insulin granule mobilization to the PM of β-cells (41). The glucose-enhanced interaction between DOC2b-GFP^{WT} and the ERM proteins was verified by co-IP, with maximum DOC2b-ERM association detectable within 2 min after glucose stimulation (Supplementary Fig. 8).

In MIN6 β-cells, ERM proteins are activated via threonine phosphorylation at the C-terminal actin-binding domain in a glucose- and calcium-dependent manner (41). A marked increase in co-IP of phosphorylated ERM (p-ERM) (>1.5-fold over basal level) with rDOC2b-GFP^{WT} in glucose-stimulated or pV-treated nondiabetic human islets suggested probable functional interaction between them (Fig. 8*Ai*). Notably, nondiabetic human islets exposed to stimulatory glucose showed a similar increase in pTyr-rDOC2b^{WT} (Fig. 8*Aii*), as did clonal β-cells. A robust increase in p-ERM–associated rDOC2b-GFP^{WT} after pV treatment in MIN6 β-cells suggests that the interaction depends on tyrosine phosphorylation (Fig. 8*B*). Increased p-ERM protein coprecipitated with rDOC2b-GFP^{WT}; and this association increased >1.5-fold following 2 min of glucose stimulation of β-cells (Fig. 8*C*). Attenuated glucose-stimulated p-ERM binding to rDOC2b-GFP^{Y301F} in the MIN6 β-cells (Fig. 8*C*) supports the concept of rapid tyrosine phosphorylation of DOC2b at Y301 to coordinate its association with p-ERM.

YES kinase depletion resulted in reduced levels of p-/activated ERM proteins in glucose-stimulated MIN6 β-cells, relative to the radixin (Supplementary Fig. 9*A* and *B*), the most abundant ERM protein in β-cell lines (41). Enrichment with rDOC2b-GFP^{WT} or rDOC2b-GFP^{Y301E}, but not rDOC2b-GFP^{Y301F}, significantly increased glucose-induced p-ERM levels, compared with the GFP control (Fig. 8*D*). Radixin knockdown (>40%) significantly attenuated DOC2b-mediated boosting of GSIS, indicating its functional requirement in this process (Supplementary Fig. 9*C* and *D*). These data supported the concept of linkages between glucose-stimulated YES kinase and DOC2b-mediated ERM protein function in the enhancement of insulin secretion in β-cells.

DISCUSSION

In this study, we uncovered a previously unknown signaling mechanism linking glucose-stimulated YES kinase to DOC2b-mediated ERM protein function in the enhancement of insulin secretion in pancreatic β-cells. We report for the first time that glucose stimulation of β-cells augments phosphorylation of DOC2b at Y301, an event that is dependent on the SFK family member YES kinase. Additionally, our study identified an interaction between DOC2b and the ERM scaffolding proteins, which is enhanced by glucose or pV and requires DOC2b Y301 phosphorylation. Moreover, our study also revealed a stimulatory effect of DOC2b enrichment on activation of ERM proteins and involvement of radixin, the ERM protein member in DOC2b-mediated GSIS boosting. Together, these observations are consistent with a new model in which stimulatory glucose triggers YES activation and targets DOC2b for phosphorylation at Y301, which facilitates DOC2b association and augmentation of p-ERM proteins and subsequent insulin release. With the ERM proteins already implicated in β-cell ISG PM localization and DOC2b known to enhance both phases of GSIS, this mechanism reveals a coupling of these processes, revealing new early upstream signaling events initiated by glucose.

IP and IB analysis. Bar graph quantification of three independent experiments shown at right. *D*, left: Representative images of MIN6 β-cells transfected with GFP or rDOC2b-GFP^{WT} or rDOC2b-GFP^{Y301F} or rDOC2b-GFP^{Y301E} for 48 h and treated with 20 mmol/L glucose for 30 min followed by IB analysis. Bar graph quantification of the IBs from three independent experiments shown at right. Anti-tubulin antibody was used as a loading control. Data are shown as mean ± SEM. *$P < 0.05$; **$P < 0.002$; ***$P < 0.0002$.

Our MD simulation showed that the flexible linker between DOC2b's C2A and C2B domains makes them highly mobile during dynamics. Comparing the modeled structures for rat and human DOC2b (as generated in MD simulation) with the recently available predicted structures from the "AlphaFold Protein Structure Database," we found that at least one of these clusters resembled the α-fold structures (Supplementary Fig. 10). Based on these, we deem the DOC2B structures to be highly dynamic and the α-fold structures capture one out of multiple possible orientations adopted by these proteins under physiological conditions.

DOC2B harbors multiple potential phosphorylation sites along its sequence. Earlier studies have demonstrated phosphorylation of Y301 and Y305 in Jurkat cells (42), Y309 in untreated human immortalized myelogenous leukemia cells (43), S411 in untreated human breast cancer tissues (44), S34 in the insulin-stimulated 3T3L-1 adipocytes (45), and Y301 in insulin-stimulated skeletal muscle cells (25). This is the first study to demonstrate phosphorylation of DOC2b and its functional significance in pancreatic β-cells. Given that glucose-stimulated tyrosine phosphorylation of DOC2b in β-cells occurs early, similar to that of Cdc42 (∼2 min after glucose stimulation) (46) but precedes the activation of PAK1 and Munc18c (maximal within 5 min of glucose stimulation) (16,46), we propose that glucose-induced DOC2b phosphorylation is one of the early events of GSIS. A lesser amount of phosphorylation of DOC2b-GFP in unstimulated cells was also observed, a phenomenon that needs further investigation to understand its functional significance.

Activation of YES by stimulatory glucose is a very early signaling event; it is maximal within 1 min of stimulation and is essential for GSIS in the β-cell (29). Until now, the only known target for YES in β-cells was Cdc42, as part of a Cdc42–Caveolin-1–PAK1 signaling pathway in second-phase GSIS (29). The current study identified YES in another early step, the glucose-stimulated tyrosine phosphorylation of DOC2b. Given the significant loss of DOC2b's boosting effect by Y301F mutation on both the first and second phases of GSIS in human islets and the targeting of Y301 by YES kinase, our study extends the understanding of YES kinase to action in biphasic GSIS in the β-cell.

Having identified YES as the proximal kinase of DOC2b in the β-cell, the next question is whether DOC2b is a direct substrate of SFK. Based on the literature, the kinetic function of SFKs is dependent on its C-terminal SH2 domain (47). Interestingly, although our co-IP analysis confirmed the binding association of DOC2b with YES kinase proteins in a stimulus-dependent manner in the β-cell, the bioinformatics study showed the absence of any SH2 binding domain (pYEEI) (47) in DOC2b. This suggests that the association of DOC2b and YES may be indirect, bridged by another factor. This is in line with the bioinformatics analysis (NetworKIN) for identification of a potential kinase for human DOC2b (Y301), which predicted an indirect interaction of human DOC2b Y301 with YES kinase (SFKs). Rho family GTPases such as Cdc42 and Rac1 (46,48) may be important for this interaction because of their involvement in glucose-induced F-actin remodeling. However, as Cdc42 is activated at approximately the same time as DOC2b (46), it is a more likely candidate than Rac1, which is activated 15–20 min after glucose stimulation (46,48). Supporting Cdc42 and C2 domain proteins interactions, previous studies have revealed that DOCK-C2 family proteins such as Dock180/Dock1 and Zizimin proteins are atypical GTP/GDP exchange factors for the small GTPases Rac and Cdc42 and are involved in cell migration and phagocytosis in eukaryotes (49). However, further investigation is required to identify factors that regulate DOC2b-YES interaction.

How glucose-stimulated and YES-mediated tyrosine phosphorylation of DOC2b might boost insulin secretion in the β-cell is an intriguing question. We previously showed that DOC2b interacts with the cytoskeletal motor protein KLC1 in skeletal muscle cells following insulin-stimulated tyrosine phosphorylation of DOC2b to enhance GLUT4 translocation (25). Our biochemical study revealed pTyr-DOC2b facilitates increased ISG abundance at the PM of the β-cell following glucose stimulation. In support of this result, our mass spectrometry data revealed the ERM family scaffolding proteins (41) as binding partners of DOC2b; co-IP analysis confirmed a glucose-stimulated increase in the $DOC2b^{WT}$-ERM/p-ERM association. Glucose- and calcium-dependent activation of the ERM proteins induces their translocation to the PM for insulin granule trafficking and docking at the cell membrane via interaction with F-actin and PIP2 (41,50). Therefore, these data support a new model in which YES-mediated tyrosine phosphorylation of DOC2b regulates GSIS via interaction with ERM proteins. Enhancement of ERM activation by pTyr-DOC2b and requirement of ERM member radixin in DOC2b-mediated GSIS boosting in β-cells support this model. Future work is required to identify the precise mechanisms linking YES-regulated DOC2b activation and DOC2b-ERM mediation of GSIS.

Acknowledgments. The authors thank Pablo A. Garcia and Erika McCown (Department of Cellular and Molecular Endocrinology, City of Hope, Duarte, CA) for technical support. Research reported in this publication also includes work performed in the Multi-omics Mass Spectrometry & Biomarker Discovery Core and the Light Microscopy/Digital Imaging Core at City of Hope. The authors also acknowledge the editorial assistance of Nancy Linford, PhD, Linford Biomedical Communications.

Funding. This study was supported by grants from the National Institute of Diabetes and Digestive and Kidney Diseases (grants DK067912, DK112917, and DK102233), the Wanek Family Project to Cure Type 1 Diabetes at the City of Hope (to D.C.T.), and JDRF postdoctoral fellowship (3-PDF-2020-934-A-N to D.C.B.). Research reported in this publication also includes work performed in the Multi-omics Mass Spectrometry & Biomarker Discovery Core and the Light Microscopy/Digital Imaging Core at City of Hope supported by the National Institutes of Health (P30CA33572). The Southern California Islet Cell Resource Center (City of Hope) and the Integrated Islet Distribution Program supplied human islets.

Duality of Interest. D.C.T. is a consultant for TrueBinding, Inc. No other potential conflicts of interest relevant to this article were reported.

Author Contributions. D.C.B. conceived of the study, researched data, contributed to the discussion, and wrote, reviewed, and edited the manuscript. A.A., S.B., E.O., and M.A. researched data, contributed to the discussion, and reviewed and edited the manuscript. D.C.T. conceived of the study, contributed to the discussion, and wrote, reviewed, and edited the manuscript. D.C.B., A.A., S.B., E.O., M.A., and D.C.T. read and approved the final version of the manuscript. D.C.T. is the guarantor of this work and, as such, had full access to all of the data in the study and takes responsibility for the integrity of the data and the accuracy of the data analysis.

Prior Presentation. Parts of this study were presented at the 81st Scientific Sessions of the American Diabetes Association, 25–29 June 2021, and the Western Region Islet Study Group meeting, Stevenson, WA, 3–5 November 2021.

References

1. Ashcroft FM, Harrison DE, Ashcroft SJ. Glucose induces closure of single potassium channels in isolated rat pancreatic beta-cells. Nature 1984;312:446–448

2. Daniel S, Noda M, Straub SG, Sharp GW. Identification of the docked granule pool responsible for the first phase of glucose-stimulated insulin secretion. Diabetes 1999;48:1686–1690

3. Rorsman P, Ashcroft FM, Trube G. Single Ca channel currents in mouse pancreatic B-cells. Pflugers Arch 1988;412:597–603

4. Satin LS, Cook DL. Voltage-gated Ca2+ current in pancreatic B-cells. Pflugers Arch 1985;404:385–387

5. Rorsman P, Braun M. Regulation of insulin secretion in human pancreatic islets. Annu Rev Physiol 2013;75:155–179

6. Mourad NI, Nenquin M, Henquin JC. Metabolic amplifying pathway increases both phases of insulin secretion independently of beta-cell actin microfilaments. Am J Physiol Cell Physiol 2010;299:C389–C398

7. Nevins AK, Thurmond DC. Glucose regulates the cortical actin network through modulation of Cdc42 cycling to stimulate insulin secretion. Am J Physiol Cell Physiol 2003;285:C698–C710

8. Orci L, Gabbay KH, Malaisse WJ. Pancreatic beta-cell web: its possible role in insulin secretion. Science 1972;175:1128–1130

9. Thurmond DC, Gonelle-Gispert C, Furukawa M, Halban PA, Pessin JE. Glucose-stimulated insulin secretion is coupled to the interaction of actin with the t-SNARE (target membrane soluble N-ethylmaleimide-sensitive factor attachment protein receptor protein) complex. Mol Endocrinol 2003;17:732–742

10. Kiraly-Borri CE, Morgan A, Burgoyne RD, Weller U, Wollheim CB, Lang J. Soluble N-ethylmaleimide-sensitive-factor attachment protein and N-ethylmaleimide-insensitive factors are required for Ca2+-stimulated exocytosis of insulin. Biochem J 1996;314:199–203

11. Lang J. Molecular mechanisms and regulation of insulin exocytosis as a paradigm of endocrine secretion. Eur J Biochem 1999;259:3–17

12. Aslamy A, Oh E, Ahn M, et al. Exocytosis protein DOC2B as a biomarker of type 1 diabetes. J Clin Endocrinol Metab 2018;103:1966–1976

13. Ke B, Oh E, Thurmond DC. Doc2beta is a novel Munc18c-interacting partner and positive effector of syntaxin 4-mediated exocytosis. J Biol Chem 2007;282:21786–21797

14. Miyazaki M, Emoto M, Fukuda N, et al. DOC2b is a SNARE regulator of glucose-stimulated delayed insulin secretion. Biochem Biophys Res Commun 2009;384:461–465

15. Ramalingam L, Oh E, Yoder SM, et al. Doc2b is a key effector of insulin secretion and skeletal muscle insulin sensitivity. Diabetes 2012;61:2424–2432

16. Jewell JL, Oh E, Bennett SM, Meroueh SO, Thurmond DC. The tyrosine phosphorylation of Munc18c induces a switch in binding specificity from syntaxin 4 to Doc2beta. J Biol Chem 2008;283:21734–21746

17. Ramalingam L, Lu J, Hudmon A, Thurmond DC. Doc2b serves as a scaffolding platform for concurrent binding of multiple Munc18 isoforms in pancreatic islet β-cells. Biochem J 2014;464:251–258

18. Friedrich R, Yeheskel A, Ashery U. DOC2B, C2 domains, and calcium: a tale of intricate interactions. Mol Neurobiol 2010;41:42–51

19. Houy S, Groffen AJ, Ziomkiewicz I, Verhage M, Pinheiro PS, Sørensen JB. Doc2B acts as a calcium sensor for vesicle priming requiring synaptotagmin-1, Munc13-2 and SNAREs. eLife 2017;6:e27000

20. Groffen AJ, Martens S, Díez Arazola R, et al. Doc2b is a high-affinity Ca2+ sensor for spontaneous neurotransmitter release. Science 2010;327:1614–1618

21. Pang ZP, Bacaj T, Yang X, Zhou P, Xu W, Südhof TC. Doc2 supports spontaneous synaptic transmission by a Ca(2+)-independent mechanism. Neuron 2011;70:244–251

22. Li J, Cantley J, Burchfield JG, et al. DOC2 isoforms play dual roles in insulin secretion and insulin-stimulated glucose uptake. Diabetologia 2014;57:2173–2182

23. Keller MP, Choi Y, Wang P, et al. A gene expression network model of type 2 diabetes links cell cycle regulation in islets with diabetes susceptibility. Genome Res 2008;18:706–716

24. Aslamy A, Oh E, Olson EM, et al. Doc2b protects β-cells against inflammatory damage and enhances function. Diabetes 2018;67:1332–1344

25. Zhang J, Oh E, Merz KE, et al. DOC2B promotes insulin sensitivity in mice via a novel KLC1-dependent mechanism in skeletal muscle. Diabetologia 2019;62:845–859

26. Kalwat MA, Wiseman DA, Luo W, Wang Z, Thurmond DC. Gelsolin associates with the N terminus of syntaxin 4 to regulate insulin granule exocytosis. Mol Endocrinol 2012;26:128–141

27. Nagano F, Orita S, Sasaki T, et al. Interaction of Doc2 with tctex-1, a light chain of cytoplasmic dynein. Implication in dynein-dependent vesicle transport. J Biol Chem 1998;273:30065–30068

28. Shimoda Y, Okada S, Yamada E, Pessin JE, Yamada M. Tctex1d2 is a negative regulator of GLUT4 translocation and glucose uptake. Endocrinology 2015;156:3548–3558

29. Yoder SM, Dineen SL, Wang Z, Thurmond DC. YES, a Src family kinase, is a proximal glucose-specific activator of cell division cycle control protein 42 (Cdc42) in pancreatic islet β cells. J Biol Chem 2014;289:11476–11487

30. Ravassard P, Hazhouz Y, Pechberty S, et al. A genetically engineered human pancreatic β cell line exhibiting glucose-inducible insulin secretion. J Clin Invest 2011;121:3589–3597

31. Giladi M, Michaeli L, Almagor L, et al. The C2B domain is the primary Ca2+ sensor in DOC2B: a structural and functional analysis. J Mol Biol 2013;425:4629–4641

32. Sastry GM, Adzhigirey M, Day T, Annabhimoju R, Sherman W. Protein and ligand preparation: parameters, protocols, and influence on virtual screening enrichments. J Comput Aided Mol Des 2013;27:221–234

33. Jacobson MP, Friesner RA, Xiang Z, Honig B. On the role of the crystal environment in determining protein side-chain conformations. J Mol Biol 2002;320:597–608

34. Maier JA, Martinez C, Kasavajhala K, Wickstrom L, Hauser KE, Simmerling C. ff14SB: improving the accuracy of protein side chain and backbone parameters from ff99SB. J Chem Theory Comput 2015;11:3696–3713

35. Horn HW, Swope WC, Pitera JW, et al. Development of an improved four-site water model for biomolecular simulations: TIP4P-Ew. J Chem Phys 2004;120:9665–9678

36. Salomon-Ferrer R, Götz AW, Poole D, Le Grand S, Walker RC. Routine microsecond Molecular Dynamics simulations with AMBER on GPUs. 2. Explicit solvent particle mesh Ewald. J Chem Theory Comput 2013;9:3878–3888

37. Roe DR, Cheatham TE 3rd. PTRAJ and CPPTRAJ: software for processing and analysis of Molecular Dynamics trajectory data. J Chem Theory Comput 2013;9:3084–3095

38. Jewell JL, Oh E, Ramalingam L, et al. Munc18c phosphorylation by the insulin receptor links cell signaling directly to SNARE exocytosis. J Cell Biol 2011;193:185–199

39. Ramalingam L, Oh E, Thurmond DC. Doc2b enrichment enhances glucose homeostasis in mice via potentiation of insulin secretion and peripheral insulin sensitivity. Diabetologia 2014;57:1476–1484
40. Nevins AK, Thurmond DC. A direct interaction between Cdc42 and vesicle-associated membrane protein 2 regulates SNARE-dependent insulin exocytosis. J Biol Chem 2005;280:1944–1952
41. Lopez JP, Turner JR, Philipson LH. Glucose-induced ERM protein activation and translocation regulates insulin secretion. Am J Physiol Endocrinol Metab 2010;299:E772–E785
42. Hornbeck PV, Kornhauser JM, Tkachev S, et al. PhosphoSitePlus: a comprehensive resource for investigating the structure and function of experimentally determined post-translational modifications in man and mouse. Nucleic Acids Res 2012;40:D261–D270
43. Luo W, Slebos RJ, Hill S, et al. Global impact of oncogenic Src on a phosphotyrosine proteome. J Proteome Res 2008;7:3447–3460
44. Mertins P, Mani DR, Ruggles KV, et al.; NCI CPTAC. Proteogenomics connects somatic mutations to signalling in breast cancer. Nature 2016;534:55–62
45. Nomiyama R, Emoto M, Fukuda N, et al. Protein kinase C iota facilitates insulin-induced glucose transport by phosphorylation of soluble nSF attachment protein receptor regulator (SNARE) double C2 domain protein b. J Diabetes Investig 2019;10:591–601
46. Wang Z, Oh E, Thurmond DC. Glucose-stimulated Cdc42 signaling is essential for the second phase of insulin secretion. J Biol Chem 2007; 282:9536–9546
47. Boggon TJ, Eck MJ. Structure and regulation of Src family kinases. Oncogene 2004;23:7918–7927
48. Wang Z, Thurmond DC. Differential phosphorylation of RhoGDI mediates the distinct cycling of Cdc42 and Rac1 to regulate second-phase insulin secretion. J Biol Chem 2010;285:6186–6197
49. Zhang D, Aravind L. Identification of novel families and classification of the C2 domain superfamily elucidate the origin and evolution of membrane targeting activities in eukaryotes. Gene 2010;469:18–30
50. Algrain M, Turunen O, Vaheri A, Louvard D, Arpin M. Ezrin contains cytoskeleton and membrane binding domains accounting for its proposed role as a membrane-cytoskeletal linker. J Cell Biol 1993;120:129–139